L_1-Adaptive based Robust Control Design for a Pressurized Water-type Nuclear Power Plant

Vineet Vajpayee, Victor Becerra, Nils Bausch, Jiamei Deng, S. R. Shimjith, A. John Arul

***Abstract*—This work presents adaptive control based design strategies for the control of a pressurized water-type nuclear power plant. An L_1-adaptive based state feedback control technique is proposed using linear quadratic Gaussian control and projection-based adaptation laws. A novel robust L_1-adaptive control technique is further proposed by integrating L_1-adaptive control with the loop transfer recovery approach to enhance the effectiveness and robustness capability. The control architecture offers robust performance and tracks the reference set-point effectively in the presence of matched and unmatched uncertainties and disturbances. The multi-input-multi-output nuclear power plant model adopted in this work is characterized by 40 state variables. The nonlinear plant model is linearised around steady-state operating conditions to obtain a linear model for controller design. The efficacy of proposed controllers is demonstrated by simulations on different subsystems of the nuclear power plant. The control performance of the proposed technique is compared with other classical control design schemes. Statistical measures are employed to quantitatively analyse controllers performance.**

***Index Terms*—Mathematical Model, Optimal control, Robust Control, Adaptive Control, Pressurized Water Reactor, Nuclear Power Plant.**

I. Introduction

A nuclear power plant (NPP) is a complex constrained nonlinear system. Control of an NPP poses challenges due to parameter variations caused by fuel burn-up, internal reactivity feedbacks, modelling uncertainties, and unknown disturbances. System parameters associated with reactor core, thermal-hydraulics, reactivity feedbacks, control rod worth, *etc*. differ considerably with operating conditions. Uncertainties in the actuator signals and noisy sensor measurements add further complexities to the control design problem. The plant control systems must be able to respond promptly and safely to fast variations in demand. Routine load cycles over a broad range of power variations can significantly affect system performance. Consequently, traditional controllers often fail to deliver desirable performance. Therefore, it is necessary to develop improved control techniques which can provide closed-loop stability in an uncertain environment and enhance the safety and operability of an NPP.

In the last two decades, various control design techniques such as state feedback assisted control (SFAC) [1]–[6], $\mathcal{H}_\infty$ control [7]–[10], model predictive control (MPC) [11]–[15], sliding mode control (SMC) [16]–[21], and different soft computing technique-based controls [22]–[31] have been proposed to deal with disturbances and uncertainties in an NPP. In the earliest work, Edwards et al. [1] proposed the idea of SFAC to enhance the local stability of the classical control loop by adding a state-feedback compensating loop. Loop transfer recovery (LTR) technique has been integrated with linear quadratic Gaussian (LQG) approach in an SFAC framework to improve reactor temperature and power controls during the variation in reactor parameters [2]–[6]. $\mathcal{H}_\infty$-based control schemes have been designed for reactor power control to obtain better robustness over the classical LQG control scheme [7]–[10]. To deal with system design constraints in an uncertain NPP system, receding horizon-based robust MPC approaches, which solve an optimization problem at each sampling instant, have been proposed [11]–[15]. SMC is another robust control design technique applied to an NPP system, which guarantees robustness to the uncertainties entering through the input channel, once the system reaches the sliding manifold [16]–[21]. However, the practical implementation of an SMC-based design is difficult, as it is susceptible to high-frequency components and sensitive to uncertainties in the reaching phase. The aforementioned model-based approaches require an accurate mathematical description of the NPP a priori for the effectiveness of the control design. Researchers have introduced robustness capabilities in the classical controllers through soft-computing techniques. Robust PID controller [22] and fractional-order PID controllers [23], [24] have been proposed to deal with system uncertainties associated with changes in operating conditions. Soft-computing based controllers such as neural network controllers [25], emotional controllers [26], fuzzy logic controllers [27]–[30], and genetic algorithms optimized controllers [31] have been proposed to study the load-following problem of nuclear reactors.

The response and the performance of an NPP differ significantly over its lifespan due to noise, component wear, parameter variations, model-plant mismatch, lack of complete physics knowledge, and other external disturbances. Thus, a constant gain control strategy designed during the commissioning of an NPP may not be suitable at a later operation stage or this may even cause an undesirable, unpredictable, or unstable response. The requirement of an accurate model becomes quite stringent, especially when retrofitting new controllers in an aged NPP.

Vineet Vajpayee (vineet.vajpayee@port.ac.uk), Victor Becerra (victor.becerra@port.ac.uk), and Nils Bausch (nils.bausch@port.ac.uk) are with School of Energy and Electronic Engineering, University of Portsmouth, Portsmouth, PO1 3DJ, United Kingdom.

Jiamei Deng (j.deng@leedsbeckett.ac.uk) is with School of Built Environment, Engineering, and Computing, Leeds Beckett University, Leeds, LS6 3QS, United Kingdom.

S. R. Shimjith (srshim@barc.gov.in) is with Reactor Control System Design Section, Bhabha Atomic Research Centre, Mumbai, 400 085, India and Homi Bhabha National Institute, Mumbai, 400 094, India.

A. John Arul (arul@igcar.gov.in) is with Probabilistic Safety, Reactor Shielding and Nuclear Data Section, Indira Gandhi Centre for Atomic Research, Kalpakkam, 603 102, India.

Thus, the control design should be adaptive to deal with these issues effectively. Hence, it is necessary to develop simple adaptive strategies which can provide closed-loop stability for an NPP. In this regard, some adaptive control approaches have been well investigated by nuclear engineering researchers [32]–[42]. In the earliest work, Park and Miley proposed an adaptive control approach to a simplified pressurized water reactor (PWR) [32]. Park and Cho applied an adaptive PID technique by tuning the feedback gains online to deal with unmodelled reactivity feedbacks in a PWR [33]. Na et al. proposed a multivariable adaptive control algorithm to control the axial flux shape in a PWR [35]. Adaptive controllers combined with soft-computing techniques like online feed-forward neural network controller [36], adaptive-fuzzy logic controller [37] and particle swarm optimized adaptive-PID controller [38] have been proposed for the power control during the load-following mode of operation. Dong et al. proposed adaptive control strategies for power-regulation using dynamic output-feedback control [39] and adaptive PID-based control [40], [41]. Recently, an adaptive feedback linearization control using SMC has been proposed for power control in a nuclear reactor [42].

Adaptive control methods require the adaptation scheme to be fast, robust, and to guarantee closed-loop stability. Model reference adaptive control (MRAC) is one of the well-known adaptive control strategies with all the features. MRAC approach has been applied to a simplified nuclear power system [34]. However, the main drawbacks of an MRAC are the occurrence of high-frequency oscillations in the control signal and the reduced tolerance to time delays, both of which can make the gain tuning difficult and can endanger the stability of the system. To resolve these issues an advanced version of MRAC, termed L_1-adaptive control was proposed by Cao and Hovakimyan [43]. The architecture of L_1-adaptive control focuses on compensating the low-frequency content of the uncertainties, as opposed to the entire frequency range compensated using MRAC. In this paper, an L_1-adaptive control strategy is proposed for a pressurized water-type nuclear power plant. An L_1-adaptive control controller consists of three parts, state predictor, adaptation law, and control design. The state predictor estimates the system states. The difference between the measured states and the predicted states is used to estimate the disturbance and update it periodically. The control design is augmented with the adaptation estimates and a low pass filter in the feedback loop to attenuate the high-frequency components in the control signal. Thus, the overall scheme provides the desired transient performance for both the systems signals, input and output, simultaneously. This paper further proposes a robust L_1-adaptive control strategy by integrating the L_1-adaptive control with the LQG/LTR approach. Thus, the overall structure has improved system performance and enhanced robustness while achieving fast adaptation. Both proposed techniques are applied to different subsystems of the PWR-type NPP.

In the literature, the coupling effects among the reactor-core, steam generator, pressurizer, turbine-governor, and different piping and plenum are ignored while designing the individual controllers. The dynamics of actuators and sensors are also omitted. Pragmatically, it is meaningful to develop control methods for the whole NPP system. However, there are very few results for controlling an entire NPP [41], [44]. On the other hand, many works assumed that the complete NPP state information is available for control design. In practice, various states are not directly available for feedback and a state estimator is required to estimate the unmeasurable states. The proposed work designs state feedback based adaptive control techniques using estimated states for the integrated NPP model. In particular, the paper addresses the following problems: the load-following mode of operation, the steam generator pressure control, the pressurizer pressure and level control, and turbine speed control. The efficacy of the proposed work has been tested using various closed-loop simulations in the MATLAB/Simulink environment. The proposed schemes have been further compared with other classical techniques. The main contributions of the paper are listed below:

- L_1-adaptive control and robust L_1-adaptive control techniques are proposed to improve system performance and robustness and to enhance set-point tracking in the presence of disturbances and uncertainties.
- Design, validation, and testing of the control strategy is performed for various control loops of a PWR-type NPP.
- The load-following operation, steam generator pressure control, pressurizer pressure and level control, and turbine speed control are studied.
- Detailed simulation analysis is done to compare the proposed technique with other classical control schemes.

The reminder of the paper is organized as follows: Section II presents the dynamic non-linear model of a PWR-type nuclear power plant. Section III formulates the control design problem. Section IV presents the proposed control scheme. Section V implements the proposed technique on the nuclear power plant model and discusses its effectiveness through simulation results. Conclusions are drawn in section VI indicating main contributions.

II. Dynamic Model of a PWR Nuclear Power Plant

The key variables of the model equations given below are described near their first occurrence, while the constant model parameters are all described, along with their units, in the nomenclature section. Typical parameter values are given in Table A.1.

A. Reactor Core Model

The core-neutronics model consisting of normalized power (P_n) and precursor concentration of six group of delayed neutrons (C_{in}) is given by,

$$\frac{dP_n}{dt} = \frac{\rho_t - \sum_{i=1}^{6} \beta_i}{\Lambda} P_n + \sum_{i=1}^{6} \frac{\beta_i}{\Lambda} C_{in}, \tag{1}$$

$$\frac{dC_{in}}{dt} = \lambda_i P_n - \lambda_i C_{in}, \qquad i = 1, 2, \ldots 6. \tag{2}$$

The neutronic power in a reactor can be monitored using ex-core detectors, placed outside the core, and their associated amplifiers. The ex-core detector current (i_{lo}) is sensed as

$$\tau_1\tau_2\frac{d^2 i_{lo}}{dt^2}+(\tau_1+\tau_2)\frac{di_{lo}}{dt}+i_{lo}=K_{lo}\log_{10}(\kappa_{lo}P_n). \quad (3)$$

The total reactivity (ρ_t) consists of reactivity due to rod movement (ρ_{rod}), and feedbacks due to variations in fuel and coolant temperatures and primary coolant pressure as

$$\rho_t=\rho_{rod}+\alpha_f T_f+\alpha_c T_{c1}+\alpha_c T_{c2}+\alpha_p p_p, \quad (4)$$

where

$$\frac{d\rho_{rod}}{dt}=Gz_{rod}. \quad (5)$$

B. Thermal-Hydraulics Model

The thermal-hydraulics model is governed by the Mann's model which relates the core power to the temperature drop from fuel (T_f) to coolant nodes (T_{c1} and T_{c2}),

$$\frac{dT_f}{dt}=H_f P_n-\frac{1}{\tau_f}(T_f-T_{c1}) \quad (6)$$

$$\frac{dT_{c1}}{dt}=H_c P_n+\frac{1}{\tau_c}(T_f-T_{c1})-\frac{2}{\tau_r}(T_{c1}-T_{cin}) \quad (7)$$

$$\frac{dT_{c2}}{dt}=H_c P_n+\frac{1}{\tau_c}(T_f-T_{c1})-\frac{2}{\tau_r}(T_{c2}-T_{c1}). \quad (8)$$

The RTDs are used to sense the coolant temperature and its transmitter at the inlet (T_{rtd1}) and outlet (T_{rtd2}) as,

$$\frac{dT_{rtd1}}{dt}=\frac{1}{\tau_{rtd}}(-T_{rtd1}+2T_{c1}-T_{rxi}) \quad (9)$$

$$\frac{dT_{rtd2}}{dt}=\frac{1}{\tau_{rtd}}(-T_{rtd2}+2T_{c2}-T_{rxu}) \quad (10)$$

A current signal (i_{rtd}) can be obtained from the sensed RTD signals as

$$i_{rtd}=K_{rtd}\frac{(((T_{rtd1}+T_{rtd2})/2)-T_{rxi0})}{(T_{rxu0}-T_{rxi0})}+4 \quad (11)$$

C. Piping & Plenum Model

Hot-leg (T_{hot}) and cold-leg (T_{cold}) pipings, reactor lower (T_{rxi}) and upper (T_{rxu}) plenums, steam generator inlet (T_{sgi}) and outlet (T_{sgu}) plenums can be represented by first order ordinary differential equations as [45],

$$\frac{dT_{rxu}}{dt}=\frac{1}{\tau_{rxu}}(T_{c2}-T_{rxu}), \quad (12)$$

$$\frac{dT_{hot}}{dt}=\frac{1}{\tau_{hot}}(T_{rxu}-T_{hot}), \quad (13)$$

$$\frac{dT_{sgi}}{dt}=\frac{1}{\tau_{sgi}}(T_{hot}-T_{sgi}), \quad (14)$$

$$\frac{dT_{sgu}}{dt}=\frac{1}{\tau_{sgu}}(T_{p2}-T_{sgu}), \quad (15)$$

$$\frac{dT_{cold}}{dt}=\frac{1}{\tau_{cold}}(T_{sgu}-T_{cold}), \quad (16)$$

$$\frac{dT_{rxi}}{dt}=\frac{1}{\tau_{rxi}}(T_{cold}-T_{rxi}). \quad (17)$$

D. Steam Generator Model

A U-tube type SG can be represented by five nodes in which, the primary coolant lump (PCL) (T_{p1} and T_{p2}) and metal tube lump (MTL) (T_{m1} and T_{m2}) are represented by two nodes each [46],

$$\frac{dT_{p1}}{dt}=\frac{1}{\tau_{p1}}(T_{sgi}-T_{p1})-\frac{1}{\tau_{pm1}}(T_{p1}-T_{m1}) \quad (18)$$

$$\frac{dT_{p2}}{dt}=\frac{1}{\tau_{p2}}(T_{p1}-T_{p2})-\frac{1}{\tau_{pm2}}(T_{p2}-T_{m2}) \quad (19)$$

$$\frac{dT_{m1}}{dt}=\frac{1}{\tau_{mp1}}(T_{p1}-T_{m1})-\frac{1}{\tau_{ms1}}(T_{m1}-T_s) \quad (20)$$

$$\frac{dT_{m2}}{dt}=\frac{1}{\tau_{mp2}}(T_{p2}-T_{m2})-\frac{1}{\tau_{ms2}}(T_{m2}-T_s). \quad (21)$$

The secondary coolant lump (SCL) represent steam pressure (p_s) by balancing mass, volume, and heat as,

$$\frac{dp_s}{dt}=\frac{1}{K_s}[U_{ms1}S_{ms1}(T_{m1}-T_s)+U_{ms2}S_{ms2}(T_{m2}-T_s) -(\dot{m}_{so}h_{ss}-\dot{m}_{fw}c_{pfw}T_{fw})]. \quad (22)$$

where,

$$K_s=m_{ws}\frac{\partial h_{ws}}{\partial p_s}+m_{ss}\frac{\partial h_{ss}}{\partial p_s}-m_{ws}\left(\frac{h_{ws}-h_{ss}}{\nu_{ws}-\nu_{ss}}\right)\frac{\partial \nu_{ss}}{\partial p_s} \quad (23)$$

E. Pressurizer Model

The water level (l_w) in the pressurizer can be obtained by applying mass balance equation on water and steam phase as,

$$\frac{dl_w}{dt}=\frac{1}{d_s A_p}\left(A_p(l-l_w)K_{2p}-\frac{C_{2p}}{C_{1p}}\right)\frac{dp_p}{dt} +\frac{1}{C_{p1}^2}\left(C_{2p}\frac{dp_p}{dt}-\dot{m}_{sur}-\dot{m}_{spr}\right)+\frac{\dot{m}_{sur}}{C_{1p}} \quad (24)$$

The pressure (p_p) can be obtained by applying volume and energy balances of water and steam mixture with steam compressibility as [47],

$$\frac{dp_p}{dt}=\frac{Q_{heat}+\dot{m}_{sur}\left(\frac{p_p\nu_s}{J_p C_{1p}}+\frac{h_{\bar{w}}}{C_{1p}}\right)+\dot{m}_{spr}\left(h_{spr}-h_w+\frac{h_{\bar{w}}}{C_{1p}}+\frac{p_p\nu_w}{J_p C_{1p}}\right)}{m_w\left(K_{3p}+\frac{K_{4p}p_p}{J_p}\right)+\frac{m_s K_{4p}p_p}{J_p}-\frac{V_w}{J_p}+\frac{C_{2p}}{C_{1p}}\left(h_{\bar{w}}+\frac{p_p\nu_s}{J_p}\right)} \quad (25)$$

where the intermediate variables are defined as,

$$C_{1p}=\frac{d_w}{d_s}-1 \quad (26)$$

$$C_{2p}=A_p(l-l_w)\frac{d_w}{d_s}K_{2p}+A_p l_w K_{1p} \quad (27)$$

$$K_{1p}=\frac{\partial d_w}{\partial p_p};K_{2p}=\frac{\partial d_s}{\partial p_p};K_{3p}=\frac{\partial h_w}{\partial p_p};K_{4p}=\frac{\partial \nu_s}{\partial p_p}. \quad (28)$$

The surge rate ($\dot{m}_{sur}$) can be represented using coolant temperatures at different nodes as

$$\dot{m}_{sur}=\sum_{j=1}^{N}V_j\vartheta_j\frac{dT_j}{dt} \quad (29)$$

F. Turbine Model

The dynamical model of a turbine consisting of the high-pressure, intermediate-pressure, and low-pressure turbines is given by [48],

$$\begin{aligned}
&\frac{d^2P_{hp}}{dt} + \left(\frac{O_{rv}+\tau_{ip}}{\tau_{hp}\tau_{ip}}\right)\frac{dP_{hp}}{dt} + \left(\frac{O_{rv}}{\tau_{hp}\tau_{ip}}\right)P_{hp} = \left(\frac{O_{rv}F_{hp}}{\tau_{hp}\tau_{ip}}\right)\bar{\dot{m}}_{so} \\
&\qquad + \left(\frac{(1+\kappa_{hp})F_{hp}}{\tau_{hp}}\right)\frac{d\bar{\dot{m}}_{so}}{dt} \\
&\frac{d^2P_{ip}}{dt} + \left(\frac{O_{rv}\tau_{hp}+\tau_{ip}}{\tau_{hp}\tau_{ip}}\right)\frac{dP_{ip}}{dt} + \left(\frac{O_{rv}}{\tau_{hp}\tau_{ip}}\right)P_{ip} = \left(\frac{O_{rv}F_{ip}}{\tau_{hp}\tau_{ip}}\right)\bar{\dot{m}}_{so} \\
&\frac{d^3P_{lp}}{dt} + \left(\frac{O_{rv}\tau_{hp}+\tau_{ip}}{\tau_{hp}\tau_{ip}} + \frac{1}{\tau_{lp}}\right)\frac{d^2P_{lp}}{dt} + \left(\frac{O_{rv}(\tau_{lp}+\tau_{hp})+\tau_{ip}}{\tau_{hp}\tau_{ip}\tau_{lp}}\right) \\
&\qquad \frac{dP_{lp}}{dt} + \left(\frac{O_{rv}}{\tau_{hp}\tau_{ip}\tau_{lp}}\right)P_{lp} = O_{rv}F_{lp}\bar{\dot{m}}_{so}
\end{aligned} \tag{30}$$

where the steam flow is $\bar{\dot{m}}_{so} = \dot{m}_{so}/\dot{m}_{sor}$, $\dot{m}_{sor}$ is the rated steam mass flow rate. The steam flow rate can be modified using the turbine-governor control valve coefficient (C_{tg}) as

$$\dot{m}_{so} = C_{tg}p_s \tag{31}$$

$$\frac{d^2C_{tg}}{dt^2} + 2\zeta_{tg}\omega_{tg}\frac{dC_{tg}}{dt} + \omega_{tg}^2C_{tg} = \omega_{tg}^2K_{tg}u_{tg} \tag{32}$$

where u_{tg} is the input signal to the valve. The total mechanical output of turbine (P_{tur}) is computed as,

$$P_{tur} = P_{hp} + P_{ip} + P_{lp}. \tag{33}$$

where P_{hp}, P_{ip}, and P_{lp} are mechanical power outputs of high-pressure, intermediate-pressure, low-pressure turbine, respectively.

The turbine-generator model also consists of a turbine speed system which produces the rate of change in turbine speed (z_{tur}) in accordance with the difference in generator demand power (P_{dem}) and turbine output as

$$\frac{dz_{tur}}{dt} = \frac{P_{tur} - P_{dem}}{(2\pi)^2 J_{tur}z_{tur}I_{tg}}. \tag{34}$$

III. Problem Formulation

Consider a linear time invariant system given by

$$\begin{aligned}
\dot{x}(t) &= Ax(t) + B_mu(t) + \sigma(t), \\
y(t) &= Cx(t)
\end{aligned} \tag{35}$$

where $x(t) \in \mathbb{R}^n$ is system state vector, $u(t) \in \mathbb{R}^m$ is control input, $y(t) \in \mathbb{R}^l$ is output, and $\sigma(t) = f\left(t, x(t), z(t)\right)$ contains process noise, modelling uncertainties, and external disturbances where $z(t) \in \mathbb{R}^p$ represents internal unmodelled dynamics. The control input is given by

$$u\left(t\right) = u_c\left(t\right) + u_a\left(t\right) \tag{36}$$

where $u_c\left(t\right)$ and $u_a\left(t\right)$ represent the nominal control and adaptive control, respectively. System (35) can be represented as,

$$\dot{x}(t) = A_mx(t) + B_m\left(\omega u_a(t) + \sigma_1(t)\right) + B_u\sigma_2(t), \tag{37}$$

where $A_m = A - B_mK_c^T \in \mathbb{R}^{n\times n}$ is state matrix. K_c is state feedback control gain. $B_m \in \mathbb{R}^{n\times m}$ is control input matrix and $B_u \in \mathbb{R}^{n\times(n-m)}$ is unmatched uncertainty input matrix such that $B_m^TB_u = 0$. $C \in \mathbb{R}^{l\times n}$ is output matrix. $\sigma_1(t) \in \mathbb{R}^m$ is matched disturbance, $\sigma_2(t) \in \mathbb{R}^{(n-m)}$ is unmatched disturbance, and $\omega \in \mathbb{R}^{m\times m}$ is uncertain system input gain matrix which denotes the cross coupling among different input. It is considered that A_m is Hurwitz, and the system (A_m, B_m) is controllable and system (A_m, C) is observable. It is assumed that $\sigma(t)$ and its partial derivatives are bounded and stable and the system input gain is partially known.

The control objective is to design an adaptive state-feedback controller to ensure that $y(t)$ tracks the output response of a desired system $M(s)$ defined as

$$M\left(s\right) = C\left(sI - A_m\right)^{-1}B_mK_g\left(s\right) \tag{38}$$

where $K_g(s)$ is a feed-forward prefilter to a given bounded piecewise-continuous reference signal.

IV. L_1-Adaptive Control Design

For the proposed technique, the total control law consists of the nominal control and the adaptive control. The nominal control is designed using state-feedback control approach and the adaptive control law is designed using the projection-based adaptation strategy. The block diagram of the proposed control scheme is depicted in Fig. 1.

A. Nominal Control Design

In this work, the nominal control is designed using LQG which involves two steps, state estimation using a Kalman filter and optimal state feedback control using LQR.

1) Kalman Filter: The Kalman filter estimation problem is to find an optimal state estimate $\hat{x}(t)$ such that the following error covariance is minimized:

$$J_1 = \lim_{t\to\infty} E\left\{\left(x - \hat{x}\right)\left(x - \hat{x}\right)^T\right\} \tag{39}$$

The Kalman filtering problem is estimated by computing the Kalman gain K_f given by

$$K_f = P_fC^T\Theta^{-1} \tag{40}$$

where P_f is a symmetric positive semidefinite matrix and can be computed using the solution of following Algebraic Riccati Equation (ARE) as

$$AP_f + P_fA^T + \Gamma\Xi\Gamma^T - P_fC^T\Theta^{-1}CP_f = 0 \tag{41}$$

where $\Gamma \in \mathbb{R}^{n\times m}$ is disturbance input matrix. Ξ and Θ are covariance of process noise and measurement noise, respectively. Thus, the estimated states $\hat{x}(t)$ for the nominal system are given by,

$$\dot{\hat{x}}(t) = A\hat{x}(t) + B_mu(t) + K_f(y(t) - C\hat{x}(t)). \tag{42}$$

2) Linear Quadratic Regulator: The LQR design computes an optimal control input by minimizing the cost function

$$J_2 = \int_0^\infty \left(\hat{x}^TQ\hat{x} + u_c^TRu_c\right)dt \tag{43}$$

where Q and R are positive semidefinite and positive definite weighing matrices, respectively. The cost function can be minimized by finding the solution of the following ARE to calculate optimal regulator feedback gain

$$A^TP_c + P_cA + Q - P_cB_mR^{-1}B_m^TP_c = 0 \tag{44}$$

where P_c is a symmetric positive semidefinite matrix. The optimal regulator feedback gain is computed as

$$K_c = R^{-1} B_m^T P_c \tag{45}$$

Thus, the state feedback control law for the system is given by,

$$u_c(t) = -R^{-1} B_m^T P_c \hat{x}(t) \tag{46}$$

The optimal state feedback control law is implemented using the estimated states.

B. Adaptive Control Design

1) Adaptation Law: For the system (37), the state predictor is given by

$$\begin{aligned} \dot{\hat{x}}(t) &= A_m \hat{x}(t) + B_m \left(\omega_0 u_a(t) + \hat{\sigma}_1(t)\right) + B_u \hat{\sigma}_2(t) \\ \hat{y}\left(t\right) &= C\hat{x}\left(t\right) \end{aligned} \tag{47}$$

where $\omega_0 = I_m$. $\hat{\sigma}_1(t)$ and $\hat{\sigma}_2(t)$ are the estimates of matched and unmatched disturbances, respectively. They can be estimated by the projection-type adaptation law [43] as

$$\begin{aligned} \dot{\hat{\sigma}}_1\left(t\right) &= \Upsilon \ \mathrm{Proj}\left(\hat{\sigma}_1\left(t\right), -\left(\tilde{x}^T\left(t\right) P_m B_m\right)^T\right), \hat{\sigma}_1\left(0\right) = \hat{\sigma}_{10} \\ \dot{\hat{\sigma}}_2\left(t\right) &= \Upsilon \ \mathrm{Proj}\left(\hat{\sigma}_2\left(t\right), -\left(\tilde{x}^T\left(t\right) P_m B_u\right)^T\right), \hat{\sigma}_2\left(0\right) = \hat{\sigma}_{20} \end{aligned} \tag{48}$$

The projection operator Proj is defined as follows [49]:

$$\mathrm{Proj}\left(\theta, v\right) = \begin{cases} v & \text{if } g\left(\theta\right) < 0 \\ v & \text{if } g\left(\theta\right) \geq 0 \text{ and } \nabla g^T v \leq 0 \\ v - \frac{\nabla g}{\|\nabla g\|} \left\langle \frac{\nabla g}{\|\nabla\| g}, v \right\rangle g\left(\theta\right) & \text{if } g\left(\theta\right) \geq 0 \\ & \text{and } \nabla g^T v > 0 \end{cases} \tag{49}$$

where ∇g is gradient of the convex function g defined as

$$g\left(\theta\right) = \frac{\left(\varepsilon_\theta + 1\right)\theta^T\theta - \theta_{\max}^2}{\varepsilon_\theta \theta_{\max}^2} \tag{50}$$

for a convex compact set with a smooth boundary given by $\Omega_c = \left\{\theta \in R^n \middle| \, g\left(\theta\right) \leq e\right\}, 0 \leq e \leq 1$, with $\theta_{\max}$ is the norm bound and $\varepsilon_\theta > 0$ is the projection tolerance. Υ is the adaptation gain, $\tilde{x}(t) = \hat{x}(t) - x(t)$, and P_m is the solution of the algebraic Lyapunov equation, $A_m^T P_m + P_m A_m = -Q_m$, for arbitrary symmetric $Q_m = Q_m^T > 0$. The adaptation law ensures that the closed-loop system is asymptotically stable by making $\tilde{x}(t) \to 0$.

The disturbance estimates, $\hat{\sigma}_1(t)$ and $\hat{\sigma}_2(t)$, can be written as

$$\begin{bmatrix} \hat{\sigma}_1(t) \\ \hat{\sigma}_2(t) \end{bmatrix} = \begin{bmatrix} \hat{\sigma}_1(kT_s) \\ \hat{\sigma}_2(kT_s) \end{bmatrix}; t \in \left[kT_s, \left(k+1\right)T_s\right] \tag{51}$$

Eq. (48) can be computed using (49) as [43],

$$\begin{bmatrix} \hat{\sigma}_1(kT_s) \\ \hat{\sigma}_2(kT_s) \end{bmatrix} = -\begin{bmatrix} I_m & 0 \\ 0 & I_{n-m} \end{bmatrix} \bar{B}^{-1} \Phi\left(T_s\right) \mu T_s \tag{52}$$

where

$$\bar{B} = \begin{bmatrix} B_m & B_u \end{bmatrix} \tag{53}$$

$$\Phi\left(T_s\right) = A_m^{-1}\left(e^{A_m T_s} - I_n\right) \tag{54}$$

$$\mu(T_s) = e^{A_m T_s} \tilde{x}(kT_s) \tag{55}$$

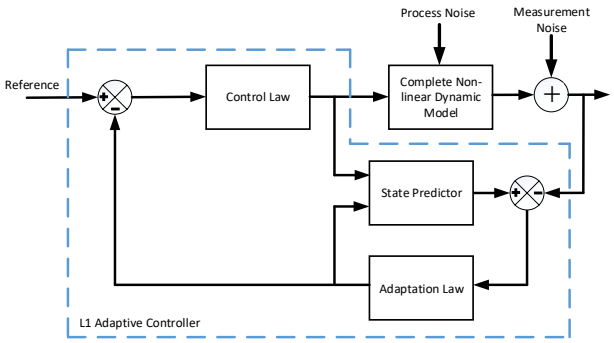

Fig. 1: Block diagram of the L_1-adaptive controller.

The estimates of disturbances are then employed to design the adaptive control law. The main advantage of projection-type adaptation law is that they prevent parameter drift in adaptation schemes.

2) Control Law: The adaptive control law is given by

$$u_a\left(s\right) = -K_a D\left(s\right)\hat{\eta}\left(s\right) \tag{56}$$

where K_a and $D(s)$ are the tuning parameters and are selected such that the transfer function $F(s)$ is strictly proper stable for all possible ω and is given by,

$$F(s) = \frac{\omega K_a D\left(s\right)}{\left(I_m + \omega K_a D\left(s\right)\right)}; F(0) = I_m \tag{57}$$

The detailed proof of stability of this type of control law can be found in [43]. $\hat{\eta}\left(s\right)$ is the Laplace transform of $\hat{\eta}\left(t\right)$ and it is given by,

$$\hat{\eta}\left(s\right) = \omega_0 u_a\left(s\right) + \hat{\eta}_1\left(s\right) + \hat{\eta}_2\left(s\right) - r_g\left(s\right) \tag{58}$$

where

$$\hat{\eta}_1\left(s\right) = \hat{\sigma}_1\left(s\right) \tag{59}$$

$$\hat{\eta}_2\left(s\right) = H_m^{-1}\left(s\right) H_u\left(s\right) \hat{\sigma}_2\left(s\right) \tag{60}$$

$$r_g\left(s\right) = K_g r\left(s\right) \tag{61}$$

The transfer function matrices H_m and H_u are defined as

$$H_m(s) = C\left(sI_n - A_m\right)^{-1} B_m \tag{62}$$

$$H_u(s) = C\left(sI_n - A_m\right)^{-1} B_u \tag{63}$$

The matched transmission zeros of $H_m(s)$ are assumed to be stable. The tuning parameters ensure that $F(s)H_m^{-1}(s)$ is a proper stable transfer function. The feed-forward prefilter K_g is chosen to decouple the signals such that $M(s)$ has off-diagonal elements with zero dc gain and diagonal element with gain one. It is given by

$$K_g = -\left(CA_m^{-1}B_m\right)^{-1} \tag{64}$$

C. Robust L_1-Adaptive Control

A robust L_1-adaptive control approach is proposed using the concept of LTR. The incorporation of a Kalman filter for state estimation weakens the robustness, stability, and performance of the nominal control. To resolve this, either the Kalman filter gain matrix or the regulator gain matrix can be modified

using the LTR approach [50]. The gains of the Kalman filter matrices are shaped so that the resultant filter transfer function has guaranteed stability margins. The open-loop system with the LQG return ratio at the input is given by

$$G(s) = K_c\left(sI - A + B_m K_c + K_f C\right)^{-1} K_f C(sI - A)^{-1} B_m \quad (65)$$

First, the LQR is designed by suitably selecting Q and R. Then, $\Gamma = B_m$, $\Xi = q\Xi$ and $\Theta = I$ are selected. The idea of LTR design is to use a fictitious gain coefficient q and then gradually increase $q \to \infty$, such that the final loop-transfer function approximates to the state-feedback loop transfer function designed by the LQR as

$$\lim_{q\to\infty} G(s) = K_c\left(sI - A\right)^{-1} B_m \quad (66)$$

The proposed robust L_1-adaptive control scheme first designs the nominal control using LQG/LTR and then integrates it with the L_1-adaptive control scheme. Thus, the integrated approach possess strong robustness capability due to LQG/LTR and the adaptive features of L_1-adaptive control.

V. Result and Discussion

The simulation results test the performance of the designed controllers under various conditions. The controllers are tested on the nonlinear PWR-type NPP model under parametric variations and matched and unmatched disturbances of ramp, sinusoidal, and chirp nature. Four important control loops are considered: reactor core power loop, steam generator loop, pressurizer loop, and turbine speed loop. In each case, the results of the proposed control schemes are compared with other classical state feedback techniques such as LQR and LQG/LTR schemes. The definition of input and output vector for every single-input-single-output control loop is given in Table I. The value of tuning parameters of the controllers for different loops is given in Table I.

A. Reactor Power Loop

The performance of the proposed controller is tested for typical load-following transients of a PWR-type NPP in the presence of disturbances and uncertainties. The disturbances and uncertainties added to the system are given by

$$\omega_1(t) = 10^{-3}\sin(2.5\times 10^{-2}t) \quad (67)$$

$$\omega_2(t) = -10^{-5}\left(r(t-300) - r(t-600) - r(t-1300) + r(t-1600)\right) \quad (68)$$

$$\omega_3(t) = \sin\left(10^{-3}\pi t + 1.98\times 10^{-5}\pi t^2\right) \quad (69)$$

where the disturbance $\omega_1(t)$ is added to the rod speed in (5), the disturbance $\omega_2(t)$ is added to total reactivity in (4), and the parametric uncertainty $\omega_3(t)$ is added to the fraction of delayed neutrons and decay constant in (1-2).

1) Case I: Initially, the NPP is assumed to be operating at 100% full power (FP). A load-following transient is considered to study typical power variations in which the reference power is varied at 6.6%/min in a ramp manner. It is given as follows:

$$P_n^{ref} = \begin{cases} 1, & 0 \le t \le 50 \\ 0.0011(t-50)+1, & 50 < t \le 250 \\ 1.22, & 250 < t \le 700 \\ -0.0011(t-700)+1.22, & 700 < t \le 900 \\ 1, & 900 < t \le 1250 \\ -0.0011(t-1250)+1, & 1250 < t \le 1450 \\ 0.78, & 1450 < t \le 1900 \\ 0.0011(t-1900)+0.78, & 1900 < t \le 2100 \\ 1, & 2100 < t \le 2500 \end{cases} \quad (70)$$

The performance of the proposed controllers, in terms of ex-core detector current corresponding to measured power is shown in Fig. 2a. The LQR and LQG/LTR controllers are unable to reject the disturbances. The outputs of L_1-adaptive control and robust L_1-adaptive control can track the variation smoothly as envisaged in the presence of uncertainties and disturbances. The robust L_1-adaptive control is found to give better set-point tracking than all other techniques. The control signal variation of control rod speed is shown in Fig. 2b. All the design approaches take similar control efforts. The L_1-adaptive control and robust L_1-adaptive control show some high-frequency components due to disturbance rejection whereas the low-frequency disturbances can be seen in the control outputs of LQR and LQG/LTR controllers.

2) Case II: Another load-following transient is considered to validate the performance during an emergency operation. The reference power value is brought down from 100% to 20% FP, to simulate an emergency operation of 80% step decrease in load. The reactor power is then slowly brought back to its initial steady-state value power at 5%/min ramp. The transient is given as follows:

$$P_n^{ref} = \begin{cases} 1.0, & 0 \le t \le 50 \\ 0.2, & 50 < t \le 500 \\ 0.05(t-500)/60 + 0.2, & 500 < t \le 1460 \\ 1.0, & 1460 < t \le 2000 \end{cases} \quad (71)$$

The purpose of such a large step transient is to test the wide-range tracking performance of the controllers. The performance of the proposed controllers in terms of ex-core detector current corresponding to measured power are shown in Fig. 2c. The LQG/LTR controller gives better performance than the LQR controller which gives large overshoot during step-load rejection. The L_1-adaptive control and robust L_1-adaptive control are able to track the sudden 80% load rejection transient without any overshoot and are able to reject the uncertainties and disturbances present in the system, out of which the robust L_1-adaptive control gives better set-point tracking. The control signal variation of control rod speed is shown in Fig. 2d. The controller signal varies sharply to track the sudden load rejection transient. The adaptive controllers show some high-frequency components due to disturbance rejection. All the control techniques are found to take similar control efforts in set-point tracking.

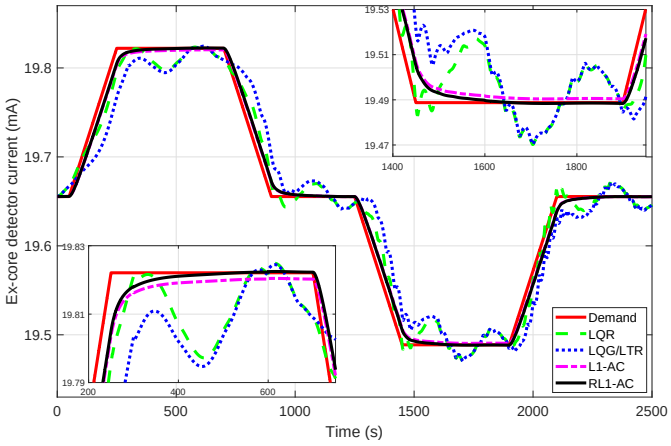

(a) Ex-core detector current.

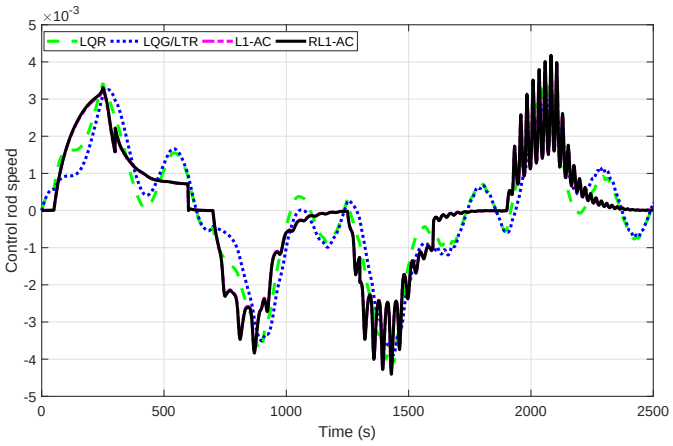

(b) Control rod speed movement.

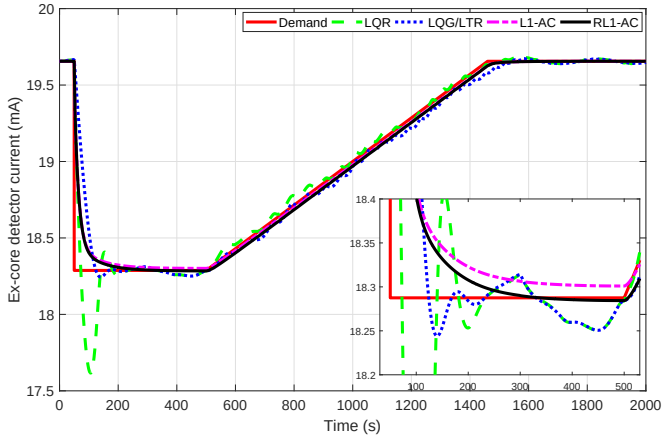

(c) Ex-core detector current.

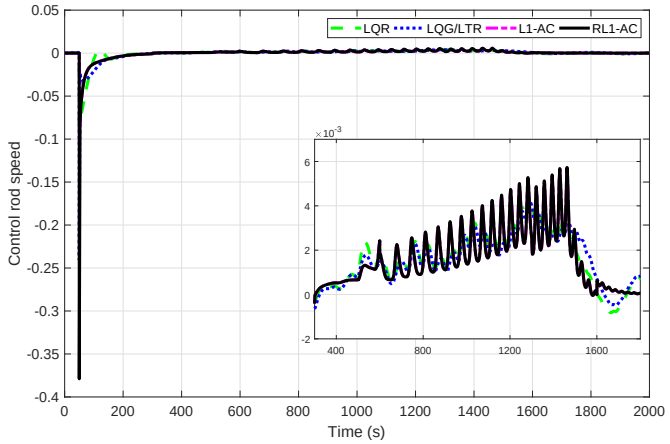

(d) Control rod speed movement.

Fig. 2: Variation of signals during load-following mode of operation.

B. Steam Generator Loop

The performance of the proposed techniques is tested for a set-point change in steam generator pressure in the presence of disturbances and uncertainties. The disturbances and uncertainties added to the system are given by

$$\omega_1(t) = 5 \times 10^{-2} \sin(10^{-3}\pi t + 9.9 \times 10^{-5}\pi t^2) \quad (72)$$

$$\omega_2(t) = 10^{-3} \sin(2.5 \times 10^{-2} t) \quad (73)$$

$$\omega_3(t) = 10^{-3} \left(r(t-20) - r(t-120) + r(t-350) - r(t-450)\right) \quad (74)$$

where the disturbance $\omega_1(t)$ is added to the input signal to the turbine governor valve in (32), the disturbance $\omega_2(t)$ is added to valve coefficient in (31), and the parametric uncertainty $\omega_3(t)$ is added added to the feed water temperature in (22).

A set point change in the secondary pressure is applied as follows:

$$p_s^{ref} = \begin{cases} 7.285, & 0 \le t \le 50 \\ 10^{-3}(t-50) + 7.285, & 50 < t \le 150 \\ 7.385, & 150 < t \le 300 \\ -10^{-3}(t-50) + 7.385, & 300 < t \le 400 \\ 7.285, & 400 < t \le 500 \end{cases} \quad (75)$$

The performance of the proposed controllers is shown in Fig. 3a. It can be observed that the L_1-adaptive control and robust L_1-adaptive control are able to track the variation smoothly in the presence of uncertainties and disturbances. On the contrary, the LQR and LQG/LTR controllers are unable to reject the disturbances. The control signal variation to turbine governor valve is shown in Fig. 3b. The LQR and LQG/LTR controllers show the low-frequency disturbance components in the control signal whereas the L_1-adaptive control and robust L_1-adaptive control give smooth variations. The control efforts taken by L_1-adaptive control and robust L_1-adaptive control are found to be lower than that of other approaches.

C. Pressurizer Loop

The pressurizer pressure control is usually achieved by actuating bank of heaters and by adjusting the spray flow rate. The disturbances and uncertainties added to the system are given by

$$\omega_1(t) = 10^3 \sin(10^{-3}\pi t + 1.998 \times 10^{-3}\pi t^2) \quad (76)$$

$$\omega_2(t) = 10 \sin(2.5 \times 10^{-1} t) \quad (77)$$

$$\omega_3(t) = -50 \left(r(t-50) - r(t-150)\right) \quad (78)$$

where the disturbances $\omega_1(t)$ and $\omega_2(t)$ are added to the input signal and to the surge flow in (25), respectively. The

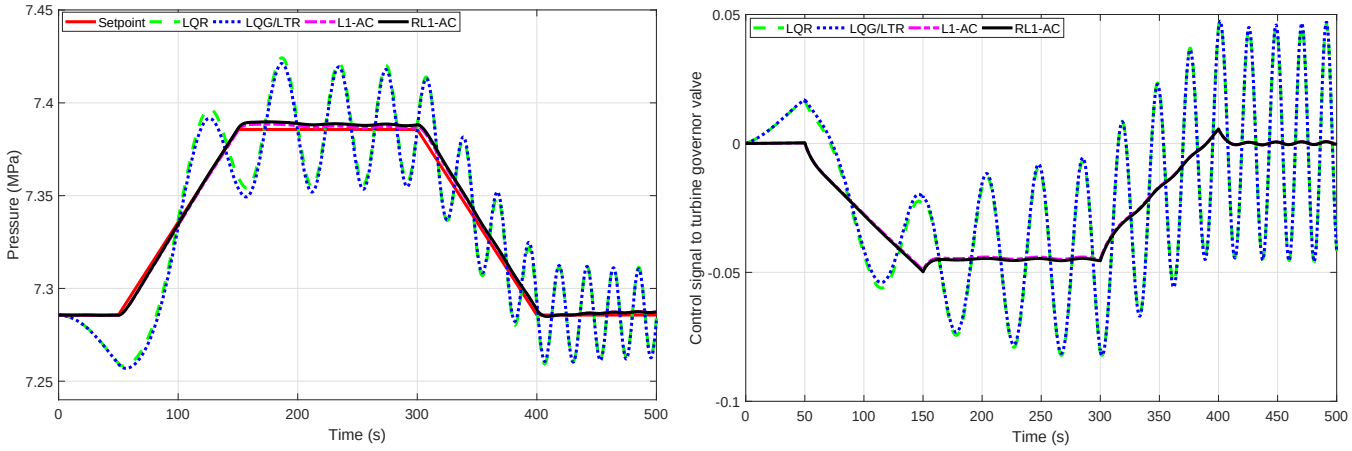

(a) Steam generator secondary pressure.

(b) Control signal to turbine governor valve.

Fig. 3: Variation of signals during a set point change in steam generator pressure.

parametric uncertainty $\omega_3(t)$ is added added to the feed water temperature in (22).

1) Pressure Control by Heater: A set point change is applied in the pressurizer pressure as follows:

$$p_p^{ref} = \begin{cases} 15.41, & 0 \leq t \leq 100 \\ 10^{-3}(t-100) + 15.41, & 100 < t \leq 200 \\ 15.51, & 200 < t \leq 250 \end{cases} \quad (79)$$

The increment in reference pressure actuates the heater system to turn on the heaters to track the pressure. The performance of the proposed controllers is shown in Fig. 4a. It can be observed that the L_1-adaptive control and robust L_1-adaptive control are able to track the variation smoothly in the presence of uncertainties and disturbances. On the contrary, the LQR and LQG/LTR controllers are unable to reject the disturbances. The rate of heat addition control signal is shown in Fig. 4b. The low-frequency disturbance components are found in the controller outputs of LQR and LQG/LTR controllers whereas the controller outputs of L_1-adaptive control and robust L_1-adaptive control contain a small amount of some high-frequency components. The L_1-adaptive control and robust L_1-adaptive control are found to take significantly lesser control efforts than the LQR and LQG/LTR approaches.

2) Pressure Control by Spray: A set-point change is applied in the pressurizer pressure as follows:

$$p_p^{ref} = \begin{cases} 15.41, & 0 \leq t \leq 100 \\ -10^{-3}(t-100) + 15.41, & 100 < t \leq 200 \\ 15.31, & 200 < t \leq 250 \end{cases} \quad (80)$$

The decrement in reference pressure actuates the spray flow system. The performance of the proposed controller is shown in Fig. 4c. It can be observed that LQR and LQG/LTR controllers are unable to handle the disturbances and uncertainties present in the system. The L_1-adaptive control and robust L_1-adaptive control are able to reject the disturbances and smoothly track the set-point variation. The rate of spray flow control signal is shown in Fig. 4d. The LQR and LQG/LTR contain the low-frequency disturbance components whereas the L_1-adaptive control and robust L_1-adaptive control contain a small amount of some high-frequency components. The L_1-adaptive control and robust L_1-adaptive control are found to require significantly lower control efforts than the LQR and LQG/LTR approaches.

3) Level Control: The pressurizer level control system maintains the water level for the reactor core coolant system. A set point change in the water level is applied as follows:

$$l_w^{ref} = \begin{cases} 28.06, & 0 \leq t \leq 50 \\ -0.05(t-50) + 28.06, & 50 < t \leq 100 \\ 25.56, & 100 < t \leq 150 \\ 0.05(t-150) + 25.56, & 150 < t \leq 200 \\ 28.06, & 200 < t \leq 250 \end{cases} \quad (81)$$

The performance of the proposed controller is shown in Fig. 4e. The L_1-adaptive control and robust L_1-adaptive control are able to track the set-point variation smoothly in the presence of uncertainties and disturbances whereas the LQR and LQG/LTR controllers are unable to reject the disturbances. The control signal to the chemical volume and control system (CVCS) is shown in Fig. 4f. The LQR and LQG/LTR contain the low-frequency disturbance components whereas the adaptive controllers contain a small amount of some high-frequency components. The L_1-adaptive control and robust L_1-adaptive control took significantly lesser control efforts.

D. Turbine Speed Loop

The turbine speed control system regulates the shaft speed by controlling the steam flow to the turbine through the turbine governor valve. The performance of the proposed technique is tested in regulating the demand power using turbine speed in the presence of disturbances and uncertainties. The disturbances and uncertainties are given by

$$\omega_1(t) = 10^{-2}\sin(0.5t) \quad (82)$$

$$\omega_2(t) = 5 \times 10^{-3}\left(\sin(0.5t) + 2\sin(t) + 3\sin(1.5t)\right) \quad (83)$$

$$\omega_2(t) = 2.5 \times 10^{5}\left(\sin(0.5t) + 2\sin(t) + 3\sin(1.5t)\right) \quad (84)$$

where the disturbance $\omega_1(t)$ is added to the input signal to the turbine governor valve in (32), the disturbance $\omega_2(t)$ is added

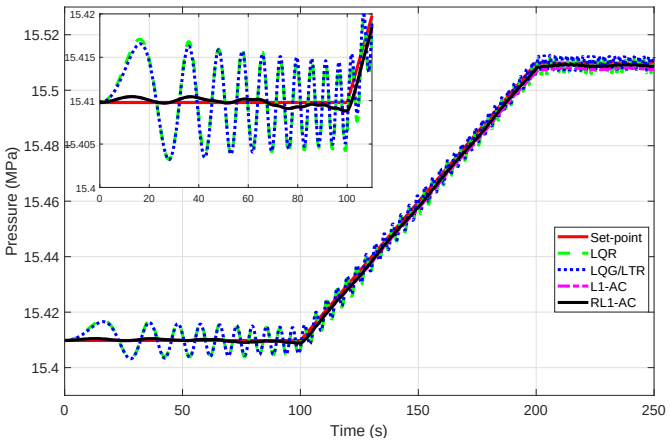

(a) Pressurizer pressure.

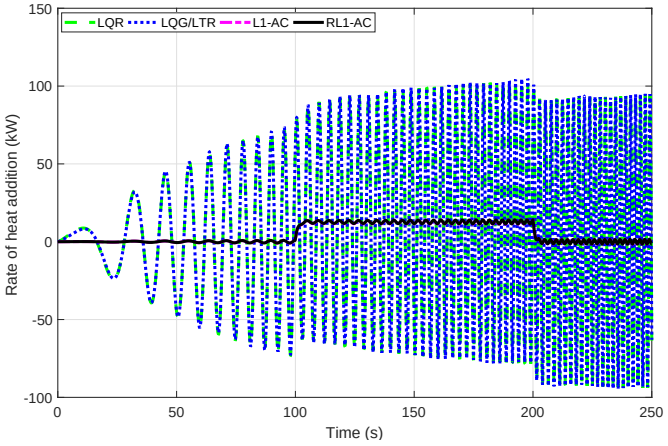

(b) Rate of heat addition.

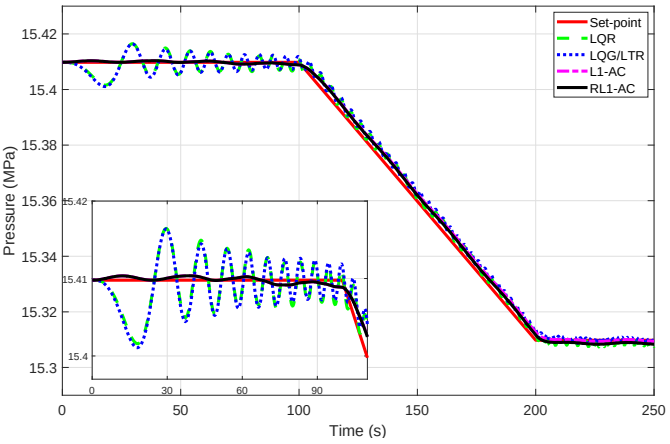

(c) Pressurizer pressure.

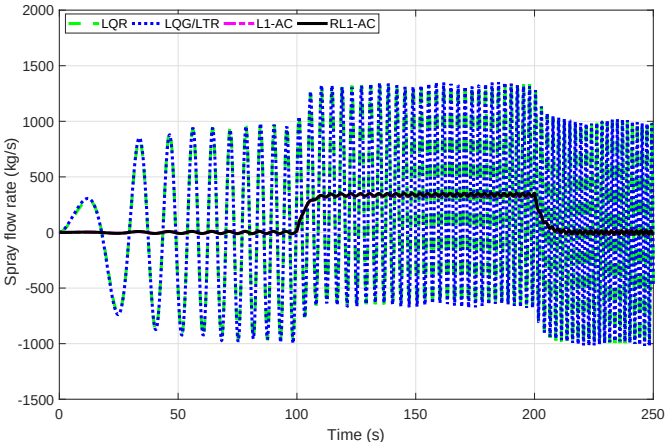

(d) Rate of spray flow.

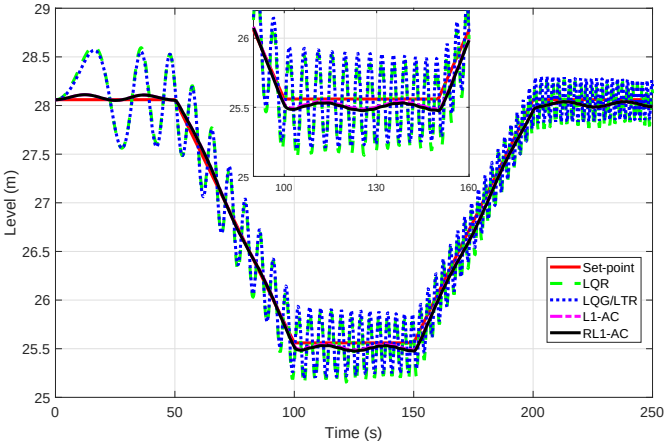

(e) Pressurizer level.

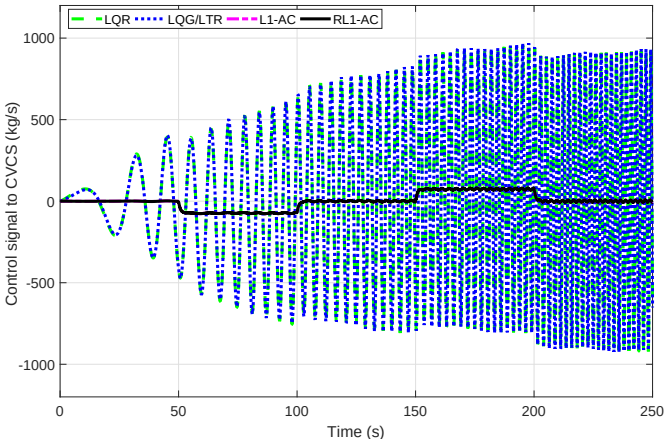

(f) Control signal to CVCS system.

Fig. 4: Variation of output and input signals during set point change in pressurizer.

to valve coefficient in (31), and the parametric uncertainty $\omega_3(t)$ is added added to the rate of heat addition in (25). The demand power from the generator is changed as follows:

$$P_{dem}^{ref} = \begin{cases} 1, & 0 \leq t \leq 10 \\ 0.0042(t-10)+1, & 10 < t \leq 50 \\ 1.168, & 50 < t \leq 250 \end{cases} \quad (85)$$

The performance of the proposed controllers for tracking the set-point change in demand power is shown in Fig. 5a. The LQR and LQG/LTR controllers track the variation with disturbances superimposed. The L_1-adaptive control and robust L_1-adaptive control controllers give better set-point tracking and they are able to handle system uncertainties and disturbances. The control signal variation to turbine governor valve is shown in Fig. 5b. It can be seen that the control effort associated with the different schemes is similar.

E. Performance Assessment

The performance of different controllers is dependent on the tuning parameters. In the case of LQR, the Q and R matrices regulate the penalties on the states variables and control input, respectively. The large value of Q results in the poles of the closed-loop system far from the origin and the state tracks the reference rapidly. On the contrary, the large value of R results in the poles of the closed-loop system close to the origin and the state tracks the reference slowly. Thus, the values of Q and R are tuned such that the set-point can be tracked quickly without any overshoot. In the case of LTR, the recovery gain q is selected based on the frequency response of the target feedback loop. The value of q is selected such that the loop transfer function approaches the ideal return ratio given by the target feedback loop. The tuning parameters of adaptive controllers are selected to ensure that the transfer function $F(s)$ is stable. The values of different tuning parameters adopted during simulations for each scheme are given in Table I.

The control performance can be statistically analysed based on the following measures. Firstly, the percentage root mean squared error (PRMSE) is calculated on the basis of tracking error. Secondly, the effect of control action on input is analysed by computing the total variation of input (TVI) and the $\mathcal{L}_2$-norm of input ($\mathcal{L}_2$NI). These are given by,

$$PRMSE = \sqrt{\frac{1}{N}\sum_{k=1}^{N}\left(y[k]-r[k]\right)^2} \times 100\%, \quad (86)$$

$$TVI = \sum_{k=1}^{N} |(u\,[k+1]-u\,[k])|, \quad (87)$$

$$\mathcal{L}_2NI = \sqrt{\sum_{k=1}^{N}\left(u[k]\right)^2}, \quad (88)$$

where N denotes the total number of samples.

Table II compares the control performance of LQR, LQG/LTR, L_1-adaptive control and robust L_1-adaptive control approaches. It is found that the values of PRMSE for the adaptive control approaches are lower than those of the other approaches at least by an order of magnitude of one in all the cases. The value of TVI and the $\mathcal{L}_2$NI are also found to be lower for the adaptive control approaches. The performance of LQG/LTR is slightly better than the LQR, however none of these techniques is able to provide the desired response in the presence of matched and unmatched disturbances and uncertainties. It can be concluded that the proposed L_1-adaptive control and robust L_1-adaptive control controllers provide better set-point tracking over other control approaches without increasing control efforts in the presence of disturbances and uncertainties.

VI. Conclusions

This work proposes state feedback-based adaptive control design strategies for the control of a pressurized water-type nuclear power plant. The proposed L_1-adaptive control designs the nominal control using the LQG technique and the adaptive control is designed using the projection-based adaptation law. The robust L_1-adaptive control technique combines the L_1-adaptive control with the loop transfer recovery technique to design an adaptive state feedback control strategy. The control architecture thus offers enhanced robustness with improved performance and tracks the reference set-point in the presence of matched and unmatched uncertainties and disturbances. The effectiveness of the techniques has been validated using simulations on different subsystems of the PWR NPP. The control performances of the proposed approaches have been quantitatively compared with LQR and LQG/LTR control approaches using different statistical measures for reactor load-following mode of operation, steam generator pressure control, pressurizer pressure and level control, and turbine speed control. The adaptive controllers can handle severe disturbances and parametric uncertainties in the system and they have been found giving better performance over other controllers.

VII. Acknowledgement

The work presented in this paper has been financially supported under grants EP/R021961/1 and EP/R022062/1 from the Engineering and Physical Sciences Research Council.

Appendix

The value of different parameters used in the model are given in Table A.1 [45]–[48].

Nomenclature

A_p	Cross-sectional area of pressurizer (m^2)
C_{in}	Normalized delayed neutron precursor concentration $(per\ unit)$
C_{tg}	Turbine governor valve coefficient
G	Reactivity worth (mK)
H	Rate of rise of temperature $({}^0C/J)$
I	Moment of inertia $(kg.m^2)$
J	Conversion factor
K	Gain
P_n	Normalized power $(per\ unit)$

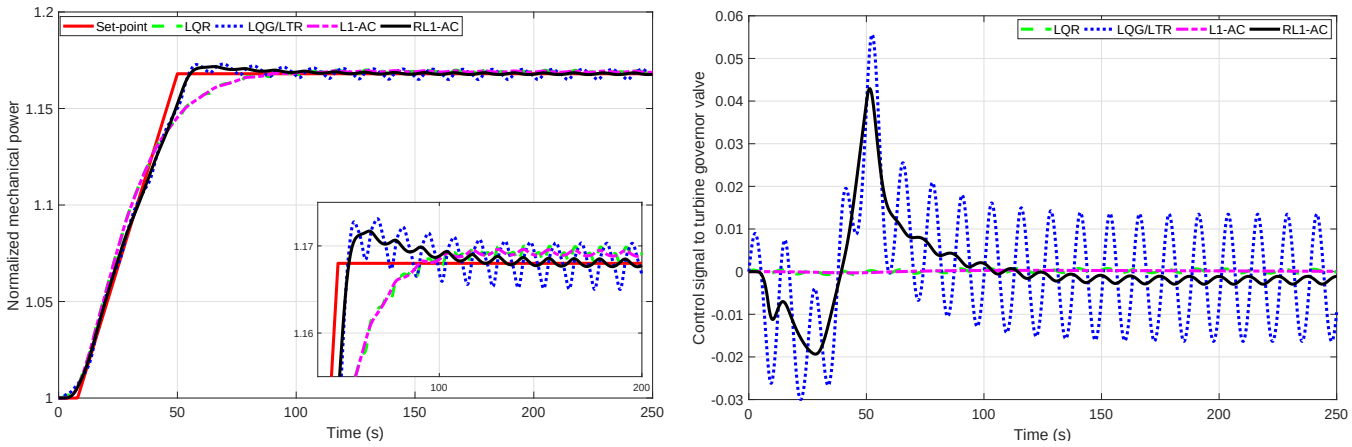

(a) Normalized mechanical power.

(b) Control signal to turbine governor valve.

Fig. 5: Variation of signals during a set point change in demand power from generator.

TABLE I: Tuning parameters for different control approaches

Configuration			LQG				LTR	L_1-adaptive	
Case	Input	Output	Q	R	Ξ	Θ	q	K_a	$D(s)$
A	z_{rod}	i_{lo}	$1\times10^{-3}I_n$	1×10^{5}	$5\times10^{-3}I_n$	1	1×10^{9}	100	$\frac{1}{0.25s+1}$
B	u_{tg}	p_s	$5\times10^{-2}I_n$	1×10^{2}	$5\times10^{-3}I_n$	1	1×10^{9}	100	$\frac{1}{0.25s+1}$
C.1	Q_{heat}	p_p	$1\times10^{0}I_n$	1×10^{-10}	$5\times10^{-5}I_n$	1	1×10^{20}	100	$\frac{1}{0.25s+1}$
C.2	$\dot{m}_{spr}$	p_p	$5\times10^{-3}I_n$	1×10^{-8}	$5\times10^{-5}I_n$	1	1×10^{15}	100	$\frac{1}{0.25s+1}$
C.3	$\dot{m}_{sur}$	l_w	$1\times10^{0}I_n$	1×10^{-6}	$5\times10^{-3}I_n$	1	1×10^{12}	500	$\frac{1}{0.25s+1}$
D	u_{tg}	z_{tur}	$1\times10^{5}I_n$	1×10^{-2}	$5\times10^{-3}I_n$	1	1×10^{9}	100	$\frac{1}{0.25s+1}$

TABLE II: Performance comparison of different control approaches

Case	Technique	PRMSE	TVI	$\mathcal{L}_2NI$
A.1	LQR	1.583×10^{0}	4.563×10^{-2}	2.569×10^{0}
	LQG/LTR	2.799×10^{0}	$\mathbf{4.131\times10^{-2}}$	$\mathbf{2.469\times10^{0}}$
	L_1	8.671×10^{-1}	8.819×10^{-2}	2.519×10^{0}
	Robust L_1	$\mathbf{8.666\times10^{-1}}$	8.926×10^{-2}	2.545×10^{0}
A.2	LQR	1.173×10^{1}	2.347×10^{-1}	1.105×10^{1}
	LQG/LTR	1.368×10^{1}	$\mathbf{2.120\times10^{-1}}$	$\mathbf{7.436\times10^{0}}$
	L_1	8.487×10^{0}	3.496×10^{-1}	9.287×10^{0}
	Robust L_1	$\mathbf{8.479\times10^{0}}$	1.310×10^{0}	9.339×10^{0}
B	LQR	2.221×10^{0}	2.050×10^{0}	2.743×10^{1}
	LQG/LTR	2.254×10^{0}	2.078×10^{0}	2.711×10^{1}
	L_1	$\mathbf{2.116\times10^{-1}}$	$\mathbf{2.620\times10^{-1}}$	$\mathbf{2.090\times10^{1}}$
	Robust L_1	2.649×10^{-1}	2.671×10^{-1}	2.114×10^{1}
C.1	LQR	3.438×10^{-1}	2.086×10^{4}	2.663×10^{4}
	LQG/LTR	3.217×10^{-1}	2.091×10^{4}	2.668×10^{4}
	L_1	1.171×10^{-1}	3.168×10^{2}	$\mathbf{3.973\times10^{3}}$
	Robust L_1	$\mathbf{1.141\times10^{-1}}$	$\mathbf{3.141\times10^{2}}$	4.017×10^{3}
C.2	LQR	2.834×10^{-1}	2.443×10^{5}	3.437×10^{5}
	LQG/LTR	3.170×10^{-1}	2.451×10^{5}	3.451×10^{5}
	L_1	1.863×10^{-1}	3.873×10^{3}	$\mathbf{1.044\times10^{5}}$
	Robust L_1	$\mathbf{1.608\times10^{-1}}$	$\mathbf{3.790\times10^{3}}$	1.055×10^{5}
C.3	LQR	2.595×10^{1}	2.007×10^{5}	2.529×10^{5}
	LQG/LTR	2.511×10^{1}	2.009×10^{5}	2.531×10^{5}
	L_1	$\mathbf{5.415\times10^{0}}$	$\mathbf{1.082\times10^{4}}$	$\mathbf{2.304\times10^{4}}$
	Robust L_1	5.745×10^{0}	1.094×10^{4}	2.312×10^{4}
D	LQR	5.368×10^{-1}	3.770×10^{-2}	1.943×10^{-1}
	LQG/LTR	3.617×10^{-1}	1.223×10^{0}	7.154×10^{0}
	L_1	5.319×10^{-1}	$\mathbf{1.103\times10^{-3}}$	$\mathbf{1.042\times10^{-1}}$
	Robust L_1	$\mathbf{3.119\times10^{-1}}$	1.787×10^{-1}	4.7043×10^{0}

Q_{heat}	Rate of heat addition (kW)
S	Effective heat transfer area (m^2)
T	Average temperature (^0C)
U	Heat transfer coefficient $(W/m^2.^0C)$
V	Volume (m^3)
c_p	Specific heat $(J/kg.^0C)$
d	Density (kg/m^3)
h	Enthalpy (J/kg)
i	Current (mA)
l	Pressurizer length (m)
m	Mass (kg)
$\dot{m}$	Mass flow rate (kg/s)
p	Pressure (MPa)
q	Torque (J/rad)
z	Speed (m/s)
Λ	Neutron generation time (s)
α	Temperature coefficient of reactivity $(^0C^{-1})$
β	Fraction of delayed neutrons
κ	Constant
λ	Decay constant (s^{-1})
ρ	Reactivity (mK)
ζ	Damping ratio
τ	Time constant (s)
ν	Specific volume (m^3/kg)
ω	Natural frequency of oscillation (rad/s)

Subscripts

$c1$, $c2$, cin	Coolant at node 1, 2 and inlet

TABLE A.1: Typical Parameters of a PWR Nuclear Power Plant

λ_1 1.2437×10^{-2}	λ_2 3.05×10^{-2}	λ_3 1.1141×10^{-1}	λ_4 3.013×10^{-1}	λ_5 1.12866	λ_6 3.0130	Λ 3×10^{-5}
β_1 2.15×10^{-4}	β_2 1.424×10^{-3}	β_3 1.274×10^{-3}	β_4 2.568×10^{-3}	β_5 7.48×10^{-4}	β_6 2.73×10^{-4}	$\partial T_{sat}/\partial p_s$ 9.47
H_f 71.8725	H_c 1.1254	τ_f 4.376	τ_c 7.170	τ_r 0.674	τ_{rxu} 2.517	τ_{rxi} 2.145
τ_{hot} 0.234	τ_{cold} 1.310	τ_{sgu} 0.726	τ_{sgi} 0.659	τ_{p1} 1.2815	τ_{p2} 1.2815	τ_{pm1} 1.2233
τ_{pm2} 1.2233	τ_{mp1} 0.3519	τ_{mp2} 0.1676	τ_{ms1} 0.3519	τ_{ms2} 0.3519	$\dot{m}_{sor}$ 2.1642×10^3	h_{ss} 2.7656×10^6
c_{pfw} 5.4791×10^3	$U_{ms1}S_{ms1}$ 1.7295×10^8	$U_{ms2}S_{ms2}$ 3.6312×10^8	m_s 2.0518×10^3	m_w 1.8167×10^4	α_f -2.16×10^{-5}	C_{tg} 2.0481
α_c -1.8×10^{-4}	α_p 1.5664×10^{-4}	τ_{rtd} 8.2	K_{rtd} 10.667	G 14.5×10^{-3}	τ_1 5×10^{-8}	τ_2 2×10^{-3}
τ_3 1	τ_4 1.01	K_{lo} 1.95692	K_{lr} 47.065	κ_{lo} 1.1067×10^{10}	ζ_{tg} 0.4933	ω_{tg} 14.6253
K_{tg} 6.25	O_{rv} 1.0	τ_{hp} 10.0	τ_{ip} 0.4	τ_{lp} 1.0	F_{hp} 0.33	F_{ip} 0
F_{lp} 0.67	κ_{hp} 0.8	d_w 595.6684	d_s 100.9506	V_w 30.4988	A_p 3.566	J_p 5.4027
l_w 8.5527	l 14.2524	h_{spr} 1.336×10^6	h_w 1.6266×10^6	$h_{\bar{w}}$ 9.7209×10^5	ν_w 1.7×10^{-3}	ν_s 9.9×10^{-3}
K_s 8.1016×10^7	J_{tur} 5.4040	I_{tg} 1.99642×10^5	$V_1\vartheta_1$ 0.5991	$V_2\vartheta_2$ 0.1814	$V_3\vartheta_3$ 0.1814	$V_4\vartheta_4$ 1.3164
$V_5\vartheta_5$ 0.2752	$V_6\vartheta_6$ 2.776	$V_7\vartheta_7$ 0.6022	$V_8\vartheta_8$ 0.6022	$V_9\vartheta_9$ 0.2776	$V_{10}\vartheta_{10}$ 0.0070	T_{fw} 232.2
K_{1p} -8.152×10^{-3}	K_{2p} 4.708×10^{-3}	K_{3p} -1.118×10^{-4}	K_{4p} 4.708×10^{-3}			

dem	Demand
f	Fuel
fw	Feed-water
hot, $cold$	Hot and cold leg
hp, ip, lp,	High, intermediate, and low pressure steam
i	i^{th} group of delayed neutron precursor
lo, lr	Logarithmic and Log rate amplifier
$m1$, $m2$	MTL 1 and 2
$mp1$, $mp2$	Transfer from MTL 1 and 2 to PCL 1 and 2
$ms1$, $ms2$	Transfer from MTL 1 and 2 to SCL
p	Pressurizer
$p1$, $p2$	PCL 1 and 2
$pm1$, $pm2$	Transfer from PCL 1 and 2 to MTL 1 and 2
rod	Regulating rod
rxi, rxu	Reactor lower and upper plenum
s	Steam
ss	Steam in secondary lump
sg, sgi, sgu	Steam generator, inlet, and outlet plenum
spr, sur	Spray and surge
$rtd1$, $rtd2$	RTD 1 and 2
tg	Turbine-Governor
tur	Turbine
w	Water
ws	Water in secondary lump

REFERENCES

[1] R. M. Edwards, K. Y. Lee, and M. A. Schultz, "State feedback assisted classical control: An incremental approach to control modernization of existing and future nuclear reactors and power plants," *Nuclear Technology*, vol. 92, no. 2, pp. 167–185, 1990.

[2] A. Ben-Abdennour, R. M. Edwards, and K. Y. Lee, "LQG/LTR robust control of nuclear reactors with improved temperature performance," *IEEE Transactions on Nuclear Science*, vol. 39, no. 6, pp. 2286–2294, 1992.

[3] H. Arab-Alibeik and S. Setayeshi, "Improved temperature control of a PWR nuclear reactor using an LQG/LTR based controller," *IEEE Transactions on Nuclear Science*, vol. 50, pp. 211–218, 2003.

[4] G. Li and F. Zhao, "Flexibility control and simulation with multi-model and LQG/LTR design for PWR core load following operation," *Annals of Nuclear Energy*, vol. 56, pp. 179 – 188, 2013.

[5] G. Li, "Modeling and LQG/LTR control for power and axial power difference of load-follow PWR core," *Annals of Nuclear Energy*, vol. 68, pp. 193 – 203, 2014.

[6] J. Wan and P. Wang, "LQG/LTR controller design based on improved SFACC for the PWR reactor power control system," *Nuclear Science and Engineering*, vol. 194, no. 6, pp. 433–446, 2020.

[7] S. G. Chi and N. Z. Cho, "H∞ control theory applied to xenon control for load-following operation of a nuclear reactor," *Nuclear Technology*, vol. 137, no. 2, pp. 127–138, 2002.

[8] H. M. Emara, A. A. Hanafy, M. M. Z. Abdelaal, and S. Elaraby, "A novel, robust control methodology application to nuclear reactors," *Nuclear Science and Engineering*, vol. 174, no. 1, pp. 87–95, 2013.

[9] G. Li, B. Liang, X. Wang, and X. Li, "Multivariable modeling and nonlinear coordination control of nuclear reactor cores with/without xenon oscillation using H∞ loop shaping approach," *Annals of Nuclear Energy*, vol. 111, pp. 82 – 100, 2018.

[10] X. Yan, P. Wang, J. Qing, S. Wu, and F. Zhao, "Robust power control design for a small pressurized water reactor using an H infinity mixed sensitivity method," *Nuclear Engineering and Technology*, 2020.

[11] A. Etchepareborda and J. Lolich, "Research reactor power controller design using an output feedback nonlinear receding horizon control method," *Nuclear Engineering and Design*, vol. 237, no. 3, pp. 268 – 276, 2007.

[12] M. G. Na, I. J. Hwang, and Y. J. Lee, "Design of a fuzzy model predictive power controller for pressurized water reactors," *IEEE Transactions on Nuclear Science*, vol. 53, no. 3, pp. 1504–1514, 2006.

[13] H. Eliasi, M. B. Menhaj, and H. Davilu, "Robust nonlinear model predictive control for nuclear power plants in load following operations with bounded xenon oscillations," *Nuclear Engineering and Design*, vol. 241, pp. 533–543, 2011.

[14] G. Wang, J. Wu, B. Zeng, Z. Xu, W. Wu, and X. Ma, "Design of a model predictive control method for load tracking in nuclear power plants," *Progress in Nuclear Energy*, vol. 101, pp. 260 – 269, 2017.

[15] V. Vajpayee, S. Mukhopadhyay, and A. P. Tiwari, "Data-driven subspace predictive control of a nuclear reactor," *IEEE Transactions on Nuclear Science*, vol. 65, no. 2, pp. 666–679, Feb 2018.

[16] R. K. Munje, B. M. Patre, S. R. Shimjith, and A. P. Tiwari, "Sliding mode control for spatial stabilization of advanced heavy water reactor," *IEEE Transactions on Nuclear Science*, vol. 60, no. 4, pp. 3040–3050, 2013.

[17] G. R. Ansarifar and M. Rafiei, "Second-order sliding-mode control for a pressurized water nuclear reactor considering xenon concentration feedback," *Nuclear Engineering and Technology*, vol. 36, pp. 94–101, 2015.

[18] G. Ansarifar and H. Akhavan, "Sliding mode control design for a PWR nuclear reactor using sliding mode observer during load following operation," *Annals of Nuclear Energy*, vol. 75, pp. 611 – 619, 2015.

[19] P. V. Surjagade, A. P. Tiwari, and S. R. Shimjith, "Robust optimal integral sliding mode controller for total power control of large phwrs," *IEEE Transactions on Nuclear Science*, vol. 65, no. 7, pp. 1331–1344, 2018.

[20] P. V. Surjagade, S. Shimjith, and A. Tiwari, "Second order integral sliding mode observer and controller for a nuclear reactor," *Nuclear Engineering and Technology*, vol. 52, no. 3, pp. 552 – 559, 2020.

[21] R. J. Desai, B. M. Patre, R. K. Munje, A. P. Tiwari, and S. R. Shimjith, "Integral sliding mode for power distribution control of advanced heavy water reactor," *IEEE Transactions on Nuclear Science*, pp. 1–1, 2020.

[22] S. Banerjee, K. Halder, S. Dasgupta, S. Mukhopadhyay, K. Ghosh, and A. Gupta, "An interval approach for robust control of a large PHWR with PID controllers," *IEEE Transactions on Nuclear Science*, vol. 62, no. 1, pp. 281–292, 2015.

[23] S. Das, I. Pan, and S. Das, "Fractional order fuzzy control of nuclear reactor power with thermal-hydraulic effects in the presence of random network induced delay and sensor noise having long range dependence," *Energy Conversion and Management*, vol. 68, pp. 200–218, 2013.

[24] S. Bhase and B. Patre, "Robust FOPI controller design for power control of PHWR under step-back condition," *Nuclear Engineering and Design*, vol. 274, pp. 20 – 29, 2014.

[25] M. N. Khajavi, M. B. Menhaj, and A. A. Suratgar, "A neural network controller for load following operation of nuclear reactors," *Annals of Nuclear Energy*, vol. 29, no. 6, pp. 751 – 760, 2002.

[26] S. S. Khorramabadi, M. Boroushaki, and C. Lucas, "Emotional learning based intelligent controller for a PWR nuclear reactor core during load following operation," *Annals of Nuclear Energy*, vol. 35, no. 11, pp. 2051 – 2058, 2008.

[27] C. Liu, J.-F. Peng, F.-Y. Zhao, and C. Li, "Design and optimization of fuzzy-PID controller for the nuclear reactor power control," *Nuclear Engineering and Design*, vol. 239, no. 11, pp. 2311 – 2316, 2009.

[28] R. Coban and B. Can, "A trajectory tracking genetic fuzzy logic controller for nuclear research reactors," *Energy Conversion and Management*, vol. 51, pp. 587–593, 2010.

[29] P. S. Londhe, B. M. Patre, and A. P. Tiwari, "Fuzzy-like PD controller for spatial control of advanced heavy water reactor," *Nuclear Engineering and Design*, vol. 274, pp. 77 – 89, 2014.

[30] M. Eom, D. Chwa, and D. Baang, "Robust disturbance observer-based feedback linearization control for a research reactor considering a power change rate constraint," *IEEE Transactions on Nuclear Science*, vol. 62, no. 3, pp. 1301–1312, 2015.

[31] S. M. H. Mousakazemi, N. Ayoobian, and G. R. Ansarifar, "Control of the reactor core power in PWR using optimized PID controller with the real-coded GA," *Annals of Nuclear Energy*, vol. 118, pp. 107 – 121, 2018.

[32] G. T. Park and G. H. Miley, "Application of adaptive control to a nuclear power plant," *Nuclear Science and Engineering*, vol. 94, pp. 145–156, 1986.

[33] M. G. Park and N. Z. Cho, "Design of a nonlinear model-based controller with adaptive PI gains for robust control of a nuclear reactor," *Progress in Nuclear Energy*, vol. 27, no. 1, pp. 37 – 49, 1992.

[34] J. D. Metzger, M. S. El-Genk, and A. G. Parlos, "Model reference adaptive control with selective state variable weighting applied to a space nuclear power system," *Nuclear Science and Engineering*, vol. 109, no. 2, pp. 171–187, 1991.

[35] M. G. Na, B. R. Upadhyaya, and J. I. Choi, "Adaptive control for axial power distribution in nuclear reactors," *Nuclear Science and Engineering*, vol. 129, no. 3, pp. 283–293, 1998.

[36] H. Arab-Alibeik and S. Setayeshi, "Adaptive control of a PWR core power using neural networks," *Annals of Nuclear Energy*, vol. 32, no. 6, pp. 588 – 605, 2005.

[37] E. Rojas-Ramrez, J. S. Bentez-Read, and A. S.-D.-L. Ros], "A stable adaptive fuzzy control scheme for tracking an optimal power profile in a research nuclear reactor," *Annals of Nuclear Energy*, vol. 58, pp. 238 – 245, 2013.

[38] S. M. H. Mousakazemi and N. Ayoobian, "Robust tuned PID controller with PSO based on two-point kinetic model and adaptive disturbance rejection for a PWR-type reactor," *Progress in Nuclear Energy*, vol. 111, pp. 183 – 194, 2019.

[39] Z. Dong, "Nonlinear adaptive power-level control for modular high temperature gas-cooled reactors," *IEEE Transactions on Nuclear Science*, vol. 60, no. 2, pp. 1332–1345, 2013.

[40] ——, "Adaptive proportional-differential power-level control for pressurized water reactors," *IEEE Transactions on Nuclear Science*, vol. 61, no. 2, pp. 912–920, 2014.

[41] Z. Dong, Y. Pan, Z. Zhang, Y. Dong, and X. Huang, "Model-free adaptive control law for nuclear superheated-steam supply systems," *Energy*, vol. 135, pp. 53 – 67, 2017.

[42] M. Zaidabadi nejad and G. R. Ansarifar, "Observer based adaptive robust feedback-linearization control for VVER-1000 nuclear reactors with bounded axial power distribution based on the validated multipoint kinetics reactor model," *Annals of Nuclear Energy*, vol. 142, no. 107380, 2020.

[43] N. Hovakimyan and C. Cao, *$\mathcal{L}1$ Adaptive Control Theory: Guaranteed Robustness with Fast Adaptation*. SIAM, 2010.

[44] G. Ablay, "A modeling and control approach to advanced nuclear power plants with gas turbines," *Energy Conversion and Management*, vol. 76, pp. 899–909, 2013.

[45] T. W. Kerlin, *Dynamic Analysis and Control of Pressurized Water Reactors*. Academic Press, 1978, vol. 14.

[46] M. R. A. Ali, *Lumped Parameter, State Variable Dynamic Models for U-tube Recirculation Type Nuclear Steam Generators*. PhD dissertation, University of Tennessee, Knoxville, 1976.

[47] M. Naghedolfeizi, *Dynamic Modeling of a Pressurized Water Reactor Plant for Diagnostics and Control*. Master's thesis, University of Tennessee, Knoxville, 1990.

[48] L. Wang, W. Sun, J. Zhao, and D. Liu, "A speed-governing system model with over-frequency protection for nuclear power generating units," *Energies*, vol. 13, no. 173, 2020.

[49] J.-B. Pomet and L. Praly, "Adaptive nonlinear regulation: estimation from the lyapunov equation," *IEEE Transactions on Automatic Control*, vol. 37, pp. 729–740, 1992.

[50] J. Doyle and G. Stein, "Multivariable feedback design: Concepts for a classical/modern synthesis," *IEEE Transactions on Automatic Control*, vol. 26, no. 1, pp. 4–16, 1981.